

**Electronic Supplementary Information for**  
**Improving Structure Stabilization of Red Phosphorus Anode**  
**via Shape Memory Effects of Ni-Ti Alloy for**  
**High-performance Sodium Ion Batteries**

**Yingtao Wang,<sup>a</sup> Xiaodan Yang,<sup>a</sup> Chenyang Zhao,<sup>a</sup> Yongliang Li,<sup>ab</sup> Hongwei Mi<sup>\*ab</sup> and**  
**Peixin Zhang <sup>\*ab</sup>**

*<sup>a</sup> College of Chemistry and Environmental Engineering, Shenzhen University, Shenzhen,  
Guangdong, 518060, PR China.*

*<sup>b</sup> Guangdong Flexible Wearable Energy and Tools Engineering Technology Research Centre  
Shenzhen University, Shenzhen, Guangdong, 518060, PR China.*

*\*Corresponding author:*

*Hongwei Mi, Tel: 86-755-26538657, Fax: 86-755-26536141, Email: [milia807@szu.edu.cn](mailto:milia807@szu.edu.cn).*

*Peixin Zhang, Tel: 86-755-26733136, Fax: 86-755-36733136, Email: [pxzhang@szu.edu.cn](mailto:pxzhang@szu.edu.cn).*

## **Experimental**

### **Preparation of Ni-Ti-P composites.**

Firstly, bulked commercial red phosphorus was ball-milled for 12 h into nanometer scale (ball-milled red-P) at a speed of 800 rpm under argon atmosphere. Ni-P and Ti-P composites were prepared through ball-milling ball-milled red-P and Ni, or Ti metal particles (200 meshes) with a particle size of 200 mesh for 10 h at 800 rpm.

For the synthesis of Ni-Ti-P composite, Ni and Ti metal were mixed and ball-milled for 2 h at 800 rpm (Ni-Ti composite). Then, Ni-Ti composite was high-temperature treated through firstly increased to 700 °C with the heating rate 10 °C min<sup>-1</sup>, then increased to 1100 °C at the heating rate of 2 °C min<sup>-1</sup>, and maintained at 1100 °C for 5 h, finally cooled down to room temperature naturally. The Ni-Ti alloy was composited with ball-milled red-P through a similar ball-milling process for 5 h at 800 rpm (Ni-Ti-P).

**Structural and physical characterization.** Field emission scanning electron microscopy (FE-SEM; JSM-7800F) was employed to observe the morphologies of the prepared materials. The crystal structure details were further characterized by transmission electron microscopy (TEM; FEI Tecnai G2 F30). The crystalline structures of the synthesized materials were observed using an Empyrean X-ray diffraction system with Cu K $\alpha$  radiation. Raman spectra were collected on an inVia Raman spectrometer using a 633 nm diode-pumped solid-state laser. The XPS tests were performed on Thermo Scientific K-Alpha<sup>+</sup>. ICP-OES (PerkinElmer; OPTIMA 7000DV) was tested to determine the contents of components of prepared materials. DSC (NETZSCH; DSC-200F3) was tested to demonstrate Martensitic transformation and inversion temperatures to verify memory effects of Ni-Ti alloy.

**Electrochemical testing.** The Electrochemical performances were tested using CR2032-type coin cells, which were assembled in an argon-filled dry glove box with the O<sub>2</sub> and H<sub>2</sub>O content under 0.1 ppm (MBraun, Inc.). The working electrodes were prepared by casting a slurry of 80 wt.% composites, 10 wt.% acetylene black, and 10 wt.% carboxymethylcellulose (CMC) binder on Cu current collector, then dried at 80 °C

under vacuum overnight, and finally cut into round film disks with the diameter of 14 mm. 1.0 M NaClO<sub>4</sub> in EC: DEC = 1:1 vol % with 5.0% FEC as additive was used as electrolyte. The sodium metal foil was used as counter electrode. Glass fiber (Grade GF/D) was used as separator. Galvanostatic charge/discharge tests were carried out on a LAND battery tester between 0.01 V and 1.5 V versus Na/Na<sup>+</sup>. The specific capacities were calculated based on red-P contents from ICP-OES results. The active material loading of Ni-Ti-P composites was calculated as 0.28 mg cm<sup>-2</sup>. The Cyclic voltammetry (CV) was performed at a scan rates of 0.1 mV s<sup>-1</sup> within the range of 0.01–1.5 V using an IVIUMnSTAT multichannel electrochemical analyser. Electrochemical impedance spectroscopy (EIS) tests were operated with the frequency range of 100, 000 and 0.1 Hz on an IVIUMnSTAT multichannel electrochemical analyser.

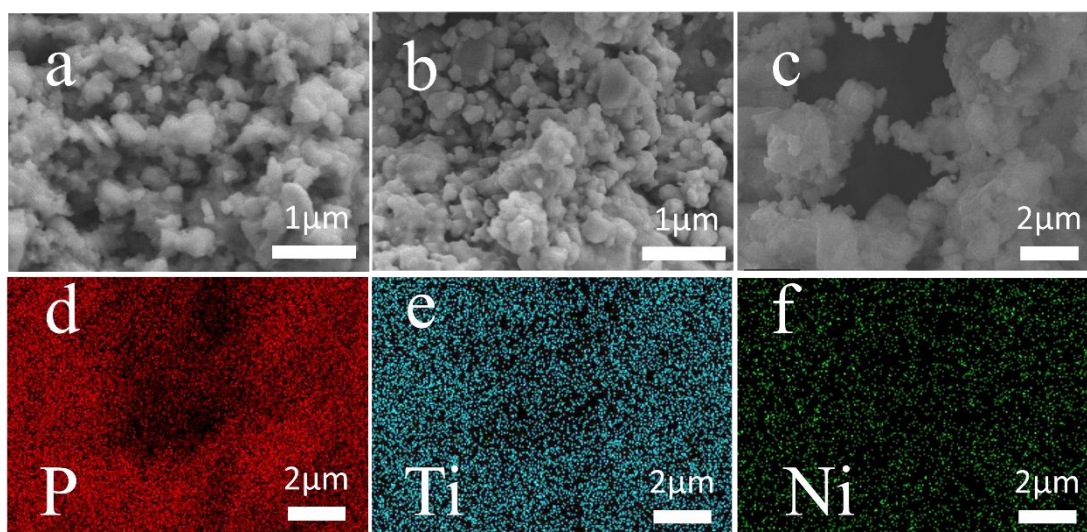


Fig. S1 SEM images of (a) Ni-P and (b) Ti-P. (c-f) SEM image and element mapping of Ni-Ti-P.

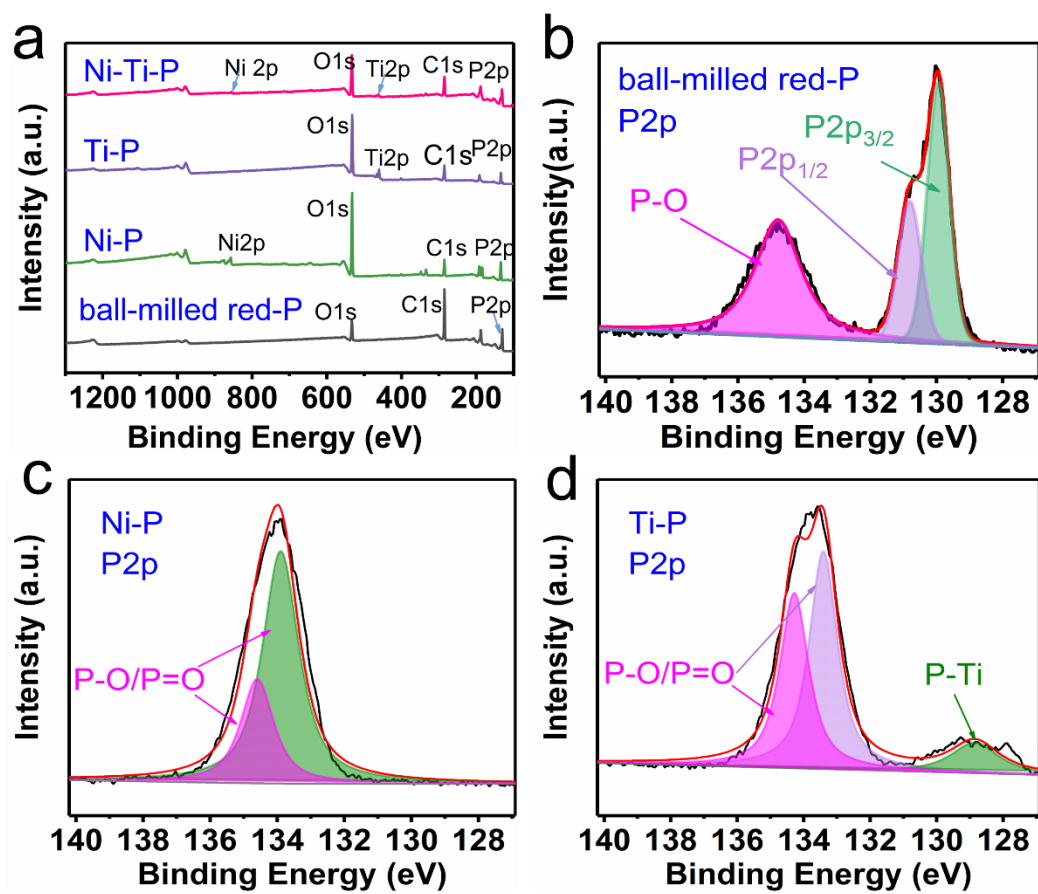


Fig. S2 (a) XPS spectra of prepared materials. The fitted P2p XPS results of (b) ball-milled red-P, (c) Ni-P, (d) Ti-P.

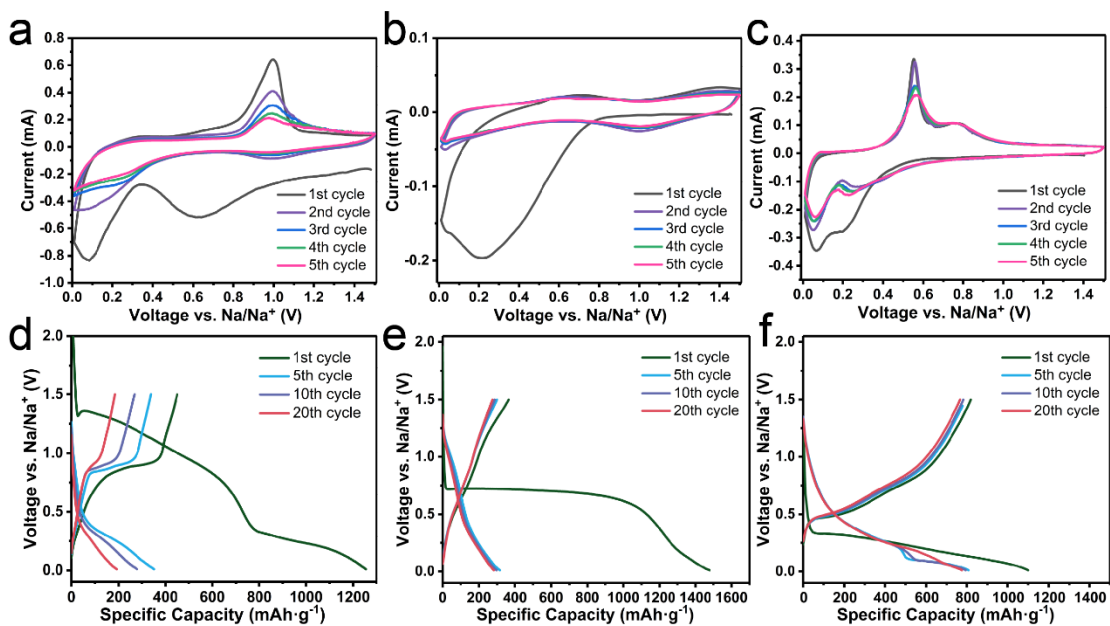


Fig. S3 Cyclic voltammograms of (a) ball-milled red-P, (b) Ni-P, (c) Ti-P at a scan rate of  $0.1 \text{ mV s}^{-1}$ . Voltage profiles of (d) ball-milled red-P, (e) Ni-P, (f) Ti-P at a current density of  $200 \text{ mA g}^{-1}$ .

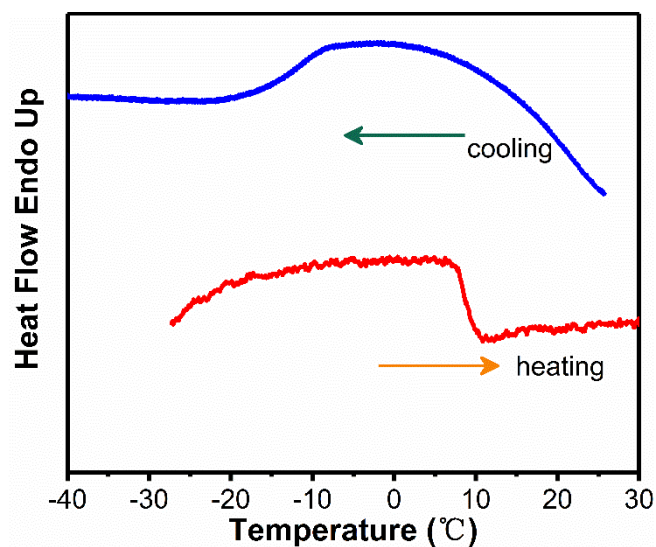


Fig. S4 Phase transition temperature curves of Ni-Ti alloy.

Table S1 Resistance values of ball-milled red-P, Ni-P, Ti-P, Ni-Ti-P composites

	$R_s$	$R_{sf}$	$R_{cf}$
Ball-milled red-P	14	190	203
Ni-P	10	705	216
Ti-P	7	259	161
Ni-Ti-P	6	132	84

Unit:  $\Omega \text{ cm}^{-2}$

Table S2 Element contents of prepared materials by ICP-OES tests

	P	Ni	Ti
Ni-Ti-P	63%	24%	13%
Ni-P	48%	52%	—
Ti-P	35%	—	65%